^{18}F-FDG PET Is an Early Predictor of Pathologic Tumor Response to Preoperative Radiochemotherapy in Locally Advanced Rectal Cancer

Giuseppe Lucio Cascini[1], Antonio Avallone[2], Paolo Delrio[3], Cesare Guida[4], Fabiana Tatangelo[5], Pietro Marone[6], Luigi Aloj[1], Francesco De Martinis[1], Pasquale Comella[2], Valerio Parisi[3], and Secondo Lastoria[1]

[1]Nuclear Medicine, IRCCS National Cancer Institute, Fondazione "G. Pascale," Naples, Italy; [2]Medical Oncology A, IRCCS National Cancer Institute, Fondazione "G. Pascale," Naples, Italy; [3]Surgical Oncology C, IRCCS National Cancer Institute, Fondazione "G. Pascale," Naples, Italy; [4]Radiotherapy, IRCCS National Cancer Institute, Fondazione "G. Pascale," Naples, Italy; [5]Pathology, IRCCS National Cancer Institute, Fondazione "G. Pascale," Naples, Italy; and [6]Surgical Endoscopy, IRCCS National Cancer Institute, Fondazione "G. Pascale," Naples, Italy

^{18}F-FDG PET is a useful tool for assessing the effects of chemo- or radiotherapy. The aim of this study was to correlate the change in tumor ^{18}F-FDG standardized uptake value (SUV) during and after preoperative radiochemotherapy, with the pathologic response achieved in locally advanced rectal cancer (LARC) patients. **Methods:** Thirty-three patients with LARC underwent total mesorectal excision after preoperative treatment, including 3 cycles of oxaliplatin, raltitrexed, 5-fluorouracil, and folinic acid during pelvic radiotherapy (45 Gy). Staging procedures included endoscopic ultrasound, MRI, and CT. ^{18}F-FDG PET scans were performed at baseline and 12 d after starting radiochemotherapy (intermediate) in all patients. Seventeen patients also had a presurgical scan. For each scan, mean and maximum SUVs were measured. The percentages of SUV decrease from baseline to intermediate (early change) and to presurgical scan (overall change) were assessed and correlated with pathologic response classified as tumor regression grade (TRG). **Results:** Eighteen tumors (55%) showed complete (TRG1) or subtotal regression (TRG2) and were classified as responders, whereas 15 cases (45%; TRG3 or TRG4) were considered nonresponders. The early median decrease of tumor SUV significantly differed between responders (−62%; range, −44% to −100%) and nonresponders (−22%; range, −2% to −48%). A significant correlation was also found between TRGs and early SUV changes ($P < 0.0001$). Responders were identified correctly by an early decrease of the mean SUV of ≥52%. **Conclusion:** This study shows that early ^{18}F-FDG PET can predict pathologic response to preoperative treatment. These findings support the usefulness of ^{18}F-FDG PET during the management with radiochemotherapy of LARC patients.

During the past decade, combined postoperative radiochemotherapy has been recommended as a standard treatment in locally advanced rectal cancer (LARC) (*1*). Advances in surgical techniques, such as total mesorectal excision (TME), have markedly improved the local control in patients with resectable rectal cancer (*2–4*). Preoperative treatment has been shown to produce a significant downsizing and downstaging of LARC, increasing the rate of complete surgical resection (*5,6*). Furthermore, a recent clinical trial demonstrated that a preoperative radiochemotherapy approach followed by TME reduced the local recurrence and improved patient tolerance compared with postoperative treatment (*7*).

Several imaging modalities are currently used for staging LARC as well as for monitoring the response to preoperative radiochemotherapy. MRI has been shown to improve the accuracy of endorectal ultrasonography (EUS) in staging the local extension, by defining the involvement of the circumferential resection margin (CRM; the smallest radial distance between the margin of the mesorectal fascia and viable tumor) (*8,9*). This information enables better definition of patients with high risk of recurrence (*10*). On the other hand, there is a low accuracy of EUS and MRI in the assessment of response to radiochemotherapy, as both techniques have been shown to be poorly reliable in differentiating viable tumor from scar or inflammatory tissue; thus, EUS and MRI have a negligible impact on predicting pathologic findings (*11,12*). A complete or subtotal pathologic

tumor response has a major impact on prognosis since it is associated with a low risk of recurrence (13,14). For this reason, the ability to predict pathologic tumor response would have a pivotal role in patient management.

^{18}F-FDG PET is a powerful, noninvasive tool for imaging tumor metabolic activity and can be used to assess changes in tumor glucose metabolism after radiation, chemotherapy, or both. The semiquantitative assessment of glucose metabolism by evaluating the standardized uptake value (SUV) has been shown to have clinical relevance in several tumor types. A strong correlation between ^{18}F-FDG SUV changes and pathologic response has been demonstrated in different cancers (15,16). Early changes in glucose metabolism, measured within 14 d after the start of preoperative radiochemotherapy, have been shown to predict response in esophageal cancer, suggesting a relevant role for ^{18}F-FDG PET in monitoring therapeutic activity (17).

Therefore, we have performed a prospective study to monitor ^{18}F-FDG PET findings during primary radiochemotherapy in LARC and correlate the observed changes with pathologic findings. The pathologic response was classified as tumor regression grade (TRG), because it has been shown to better define tumor regression after primary radiochemotherapy (18).

MATERIALS AND METHODS

Patient Selection

Thirty-three consecutive patients (20 men, 13 women) with a median age of 58 y (range 29–74), were recruited in this study (Table 1). All patients had a biopsy-proven rectal adenocarcinoma. EUS, MRI of the liver and pelvis (with endorectal contrast media), CT of the abdomen and pelvis, and chest x-ray were used as staging procedures. Patients with clinical T4, or nodal involvement, or

TABLE 1
Patient Characteristics, Clinical Staging, Histopathologic Findings, and Tumor ^{18}F-FDG SUV-mean Changes

Patient no.	Sex	Age (y)	cTNM	cMRC	GR	Tumor location	pTNM	TRG	R status	Baseline	Intermediate	Before surgery	Early change (%)	Overall change (%)
1	F	29	T4 N2	≤5 mm	High	≤5 cm	T4 N0	4	R1	4.15	3.54	2.74	14.69	33.9
2	F	66	T3 N0	>5 mm	Interm.	≤5 cm	T1 N0	2	R0	10.6	4.5	NP	57.60	
3	M	69	T3 N1	≤5 mm	Mod. high	≤5 cm	T0 N0	1	R0	16.2	4.25	NM	73.76	100.0
4	F	57	T2 N1	>5 mm	Interm.	≤5 cm	T2 N0	4	R0	4.75	4.28	NM	9.89	100.0
5	F	73	T3 N1	>5 mm	Mod. high	>5 cm	T0 N0	1	R0	4.06	1.26	NP	68.90	
6	M	60	T4 N1	≤5 mm	High	≤5 cm	T3 N1	3	R1	4.68	4.57	NP	2.35	
7	M	74	T3 N0	≤5 mm	Interm.	>5 cm	T0 N0	1	R0	5.37	1.89	NP	64.80	
8	M	48	T3 N1	NP	Mod. high	>5 cm	T3 N1	3	R0	8.03	7.35	NP	8.46	
9	M	67	T3 N1	≤5 mm	Mod. high	>5 cm	T0 N0	1	R0	7.37	1.91	NP	74.00	
10	M	48	T3 N2	≤5 mm	High	>5 cm	T0 N0	1	R0	4.97	2.12	NM	57.34	100.0
11	M	66	T3 N1	>5 mm	Mod. high	>5 cm	T0 N0	1	R0	10.03	3.21	NM	67.98	100.0
12	F	40	T3 N2	>5 mm	High	>5 cm	T2 N2	3	R0	11.7	9.1	6.3	22.20	46.2
13	M	70	T3 N1	NP	Mod. high	>5 cm	T2 N1	3	R0	7.19	3.76	NM	47.70	100.0
14	M	53	T3 N1	>5 mm	Mod. high	>5 cm	T2 N0	3	R0	4.55	4.03	2.01	11.42	55.8
15	F	42	T3 N1	>5 mm	Mod. high	>5 cm	T0 N1	1	R0	9.52	3.62	2.07	61.97	78.3
16	M	58	T3 N1	>5 mm	Mod. high	>5 cm	T0 N0	1	R0	6.7	2.21	NM	67.01	100.0
17	F	30	T3 N1	≤5 mm	Mod. high	>5 cm	T0 N0	1	R0	9.08	NM	NP	100.00	
18	M	50	T3 N1	≤5 mm	Mod. high	≤5 cm	T3 N1	3	R0	3.2	3.08	2.17	3.75	32.2
19	F	50	T3 N0	≤5 mm	Interm.	≤5 cm	T2 N0	3	R0	6.34	3.94	2.11	37.85	66.0
20	F	52	T3 N1	≤5 mm	Mod. high	≤5 cm	T2 N0	2	R0	6.8	3.02	2.1	55.58	67.6
21	F	64	T3 N1	≤5 mm	Mod. high	>5 cm	T3 N0	3	R0	7.68	4.85	2.52	36.84	67.1
22	M	67	T3 N1	>5 mm	Mod. high	≤5 cm	T3 N0	3	R0	8.03	6.23	NP	22.41	
23	M	47	T3 N2	≤5 mm	High	≤5 cm	T2 N0	2	R0	11.23	4.64	NP	58.68	
24	M	53	T3 N2	≤5 mm	High	≤5 cm	T3 N0	2	R0	8.87	3.62	NP	59.18	
25	F	66	T3 N1	≤5 mm	Mod. high	>5 cm	T3 N0	3	R0	10.69	7.55	NP	29.37	
26	F	58	T3 N1	NP	Mod. high	≤5 cm	T0 N0	1	R0	10.54	3.22	NP	69.44	
27	M	69	T3 N1	≤5 mm	Mod. high	≤5 cm	T3 N1	2	R0	13.75	5.67	NP	58.76	
28	F	65	T4 N2	≤5 mm	High	>5 cm	T3 N1	3	R0	10.87	7.19	NP	33.85	
29	M	64	T3 N0	≤5 mm	Interm.	≤5 cm	T2 N0	3	R0	8.39	6.19	NP	26.22	
30	M	41	T4 N0	≤5 mm	Mod. high	≤5 cm	T2 N0	3	R0	9.67	7.21	NP	25.43	
31	M	62	T2 N1	>5 mm	Interm.	>5 cm	T1 N1	2	R0	6.3	2.4	NM	61.90	100.0
32	M	49	T3 N2	≤5 mm	High	>5 cm	T0 N0	1	R0	18.58	5.43	NM	70.75	100.0
33	M	36	T3 N0	≤5 mm	Interm.	≤5 cm	T0 N0	1	R0	6.32	2.68	NM	57.6	100.0

cTNM = clinical TNM; cCRM = clinical CRM; pTNM = pathologic TNM; R status = resection status; R0 = macroscopically complete resection; R1 = minimal residue resection; GR = Gunderson risk classification (19); Interm = intermediate; Mod. high = moderately high; NM = not measurable; NP = not performed.

T3 N0 with a tumor location of ≤5 cm from the anal verge or a CRM of ≤5 mm, defined by MRI, were enrolled.

On the basis of the clinical staging, they were stratified according to the risk of recurrence of Gunderson et al. (*19*) as follows: 7 intermediate risk, 18 moderately high risk, and 8 high risk.

The clinical CRM was ≤5 mm in 20 patients, whereas it was >5 mm in 10 cases. In 3 patients, MRI was not performed because of the presence of a metal prosthesis or of metallic stitches. The tumor was located <5 cm from the anal verge in 16 patients.

All of these patients were taking part in a phase I−II trial of preoperative radiochemotherapy (*20*), which was approved by the Independent Ethical Committee of the National Cancer Institute of Naples, and all patients gave written informed consent to participate in this trial.

Preoperative Radiochemotherapy

Radiotherapy was performed using a 3-field technique (posteroanterior and 2 lateral fields).

Standard fractions of 1.8 Gy/d to the reference point were given 5 times a week up to a total dose of 45 Gy. The clinical target volume encompassed the tumor and the whole mesorectum, the common and internal iliac nodes, and the pelvic nodes plus a 1.5-cm margin. Multileaf collimator shielding was always used to protect the small bowel and the bone marrow. A 3-dimensional plan was performed with a dedicated treatment planning system after online CT virtual simulation.

The preoperative concomitant chemotherapy consisted of 3 biweekly cycles of oxaliplatin as a 2-h intravenous infusion and raltitrexed as a 15- min intravenous infusion on day 1, and folinic acid (LFA) intravenously over 2 h followed by 5-fluorouracil (5FU) as an intravenous bolus on day 2 on the first, third, and fifth week of radiotherapy. All patients received the same dose level of the planned combination regimen, which included oxaliplatin (100 mg/m^2), raltitrexed (2.5 mg/m^2), LFA (250 mg/m^2), and 5FU (900 mg/m^2).

PET

^{18}F-FDG PET scans were planned before (baseline) and 12 d after the beginning of combination treatment (intermediate). In 17 patients an additional ^{18}F-FDG PET scan was performed after radiochemotherapy, a few days before surgery (presurgical). PET studies (ECAT EXACT 47; Siemens) were acquired in 2-dimensional whole-body mode 60 min after the administration of 300−385 MBq using 4-min emission and 1-min transmission acquisitions for each bed position. The patients fasted for at least 6 h, and the blood glucose level was <150 mg/dL. Image data were reconstructed into a 128 × 128 matrix, with the ordered-subsets expectation maximization algorithm (2 iterations, 16 subsets). The emission data were corrected for decay, dead time, random coincidences, and measured photon attenuation.

Irregular regions of interest (ROIs) were semiautomatically drawn by the same investigator on transaxial planes using a dedicated workstation and software (e.soft version 4.0.8.15; Siemens), using a region-growing method that included pixels above a threshold value (typically set between 20% and 50% of the maximum pixel value), which was defined to include all viable tumor within lesion margins. The process required intervention by the investigator only for the rough definition of the tumor area and for setting the threshold values. For each tumor volume, both the maximum SUV (SUV-max) and the mean SUV (SUV-mean) were calculated as follows: SUV = (measured activity concentration [Bq/mL])/(injected activity [Bq]/body weight [kg] × 1,000). SUV-max was considered as the maximum value measured in the visualized lesion, whereas SUV-mean was determined from the average activity values in the ROIs.

The analysis of ^{18}F-FDG PET results was performed by comparison of the metabolic activity in the rectal lesion at baseline, intermediate, and presurgical scans (when performed), and the changes were expressed as the percentage of SUV reduction, by dividing the the intermediate by baseline SUV (early change), presurgical by intermediate SUV (late change), and presurgical by baseline (overall change). Complete resolution of ^{18}F-FDG uptake in the tumor so that it was indistinguishable from normal surrounding tissue was considered a complete metabolic response; therefore, a 100% reduction of metabolic activity was assumed.

Surgical Approach and Evaluation of Pathologic Response

Patients underwent TME 8 wk after completing radiochemotherapy. An anterior resection or an abdominoperineal resection was performed on the basis of the results of restaging.

The surgical specimens containing the tumor were processed and evaluated by a pathologist who was unaware of the clinical and PET findings. CRM was examined by sampling a 1-mm-thick slice (*21*) and defined as positive if tumor residuals were found ≤1 mm from the margin. Lymph nodes were searched by the manual dissection method (*22*).

Tumor regression was evaluated according to the TRG score (*23*) as follows: TRG1, complete response with absence of residual cancer and fibrosis extending through the wall; TRG2, presence of residual cancer cells scattered through the fibrosis; TRG3, increase in the number of residual cancer cells, with fibrosis predominant; TRG4, residual cancer outgrowing fibrosis; TRG5, absence of regressive changes. Tumors with a TRG1 or a TRG2 score were considered responders, whereas remaining tumors (TRG3, TRG4, and TRG5) were classified as nonresponders.

Statistical Analysis

The statistical analyses were performed using SPSS software (version 12; SPSS Inc.). The quantitative values were expressed as median and range. The comparison of individual SUV changes over time was performed using the Wilcoxon signed-rank test. Differences in SUV-max and SUV-mean between pathologic responders and nonresponders were evaluated using the Mann–Whitney test.

The ^{18}F-FDG uptake observed in the baseline, intermediate, and presurgical scans was correlated with the TRG groups using the Kruskal–Wallis test. The same test was also applied to compare the SUV values and SUV changes with the Gunderson risk strata, CRM status, tumor location, and TRGs.

The receiver-operator-characteristic (ROC) curves were plotted for both SUV-mean and SUV-max changes to evaluate accuracy (test variable) for the prediction of the pathologic response (state variable), and the optimal threshold value (the one yielding the highest sensitivity and specificity) was identified to differentiate responders from nonresponders.

RESULTS

Pathologic Results

All patients had an intact complete mesorectum, and a mean of 31 nodes was retrieved. According to the TRG classification, TRG1 was achieved in 12 patients, TRG2 in

6 patients, TRG3 in 13 patients, and TRG4 in 2 patients. No patient was graded as TRG5. Pathologic response according to the clinical stage is reported in Table 2. Interestingly, all but 1 of the TRG1 tumors had a pN0 stage, whereas a single micrometastatic focus was detected in patient 15. In summary, according to the TRG findings, 18 patients (55%) were classified as responders and 15 patients were classified as nonresponders.

A downstaging of the T level was observed in 24 of 33 patients (73%), and the lymph node involvement was reduced in 19 of 27 patients (70%). The occurrence of a pathologic response was not statistically different in the Gunderson risk strata ($P = 0.78$). Similarly, tumor location and clinical CRM were not related to the pathologic findings.

A complete resection (R0) was achieved in all responder patients. In contrast, a microscopically positive resection (R1) was observed in 2 of 15 nonresponder patients.

Time Course of ^{18}F-FDG Uptake and Correlation with Clinical Staging

In all patients, intense ^{18}F-FDG uptake within the tumor was detected on the baseline scan, with a median SUV-max of 11.20 (range, 5.30–36.90) and a median SUV-mean of 8.3 (range, 3.20−18.58). No significant relationship between SUVs and Gunderson risk strata, clinical CMR status, or tumor location was found.

A reduction of glucose metabolism was measured in all patients 12 d after the start of radiochemotherapy ($P < 0.0001$). Patient 17 showed a complete metabolic response (100% reduction). In the remaining 32 patients, SUV-max ranged from 1.9 to 11.3 (median, 6.0); the SUV-mean ranged from 1.9 to 9.1 (median, 4.0).

Early changes in SUV-max and SUV-mean were extremely variable, ranging from −1% to −100% for SUV-max and from −2% to −100% for SUV-mean (Table 1). Median values were −50% and −56%, respectively. No statistical correlation was observed between early change and the Gunderson risk strata, CMR status, or tumor location.

Moreover, in the 17 patients who had a preoperative PET scan, a further reduction of ^{18}F-FDG uptake was observed ($P = 0.012$). Complete metabolic response was found in 9 of

17 patients. In the remaining 8 patients, the median value of SUV-max was 2.7 (range, 2.4−8.3) and of SUV-mean was 2.1 (range, 2.0−6.3). The median value of the late change for the entire group was −100% for SUV-max (range, −19% to −100%) and −100% for SUV-mean (range, −22% to −100%). Moreover, diffuse rectal ^{18}F-FDG uptake, with no focal hot spots, was noted in 5 patients. This appeared to be related to postradiotherapy changes occurring in tissues surrounding the tumor. Persistent intense ^{18}F-FDG tumor uptake at the end of treatment was observed in only 1 patient (patient 12, Table 1: SUV-max of 8.3 and SUV-mean of 6.3), in whom a poor early change was observed as well.

The time course of ^{18}F-FDG SUV-max and SUV-mean values is summarized in Figure 1.

Time Course of ^{18}F-FDG Uptake and Correlation with Pathologic Staging

The TRG groups were not statistically related with the baseline SUV values ($P = 0.2$), whereas a significant correlation was observed with the intermediate SUV values (SUV-max, $P = 0.009$; SUV-mean, $P = 0.003$). An even more significant correlation was observed between TRGs and the early SUV changes ($P < 0.0001$ for both SUV-max and SUV-mean). Tumors classified as TRG1 showed a median early change of −66% (range, −44% to −100%) for SUV-max and of −68% (range, −57% to −100%) for SUV-mean. Corresponding median values were −55% (range, −48% to −71%) and −59% (range, −56% to −62%) for TRG2. In TRG3, the median early change was −29% (range, −1% to −63%) for SUV-max and −25% (range, −2% to −48%) for SUV-mean. In TRG4, a very scant early change was observed both for SUV-max (median, −3%; range, −1% to −4%) and for SUV-mean (median, −12%; range, −10% to −15%) (Fig. 2).

Consequently, in responding tumors, the median early change was −62% (range, −44% to −100%) for SUV-max and −63% (range, −56% to −100%) for SUV-mean, whereas, among nonresponders, the median early change was −28% (range, −1% to −63%) for SUV-max and −22% (range, −2% to −48%) for SUV-mean ($P < 0.0001$ for both

TABLE 2
Pathologic Response Among Different Clinical Stages

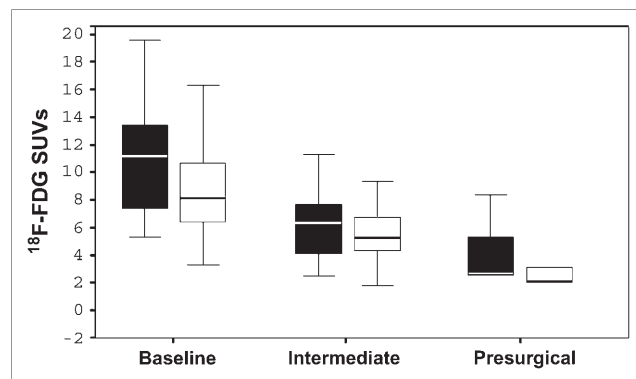| Clinical TN (n)	Pathologic TN (n)	TRG (n)
T2N1 (2)	T1N1 (1), T2N0 (1)	TRG2 (1), TRG4 (1)
T3N0 (5)	T0N0 (2), T1N0 (1), T2N2 (2)	TRG1 (2), TRG2 (1), TRG3 (2)
T3N1 (17)	T0N0 (7), T0N1 (1), T2N0 (2), T2N1 (1), T3N0 (3), T3N1 (3)	TRG1 (8), TRG2 (2), TRG3 (7)
T3N2 (5)	T0N0 (2), T2N0 (1), T2N2 (1), T3N0 (1)	TRG1 (2), TRG2 (2), TRG3 (1)
T4N0 (1)	T2N0	TRG3 (1)
T4N1 (1)	T3N1	TRG3 (1)
T4N2 (2)	T3N1 (1), T4N0 (1)	TRG3 (1), TRG4 (1)

FIGURE 1. Relative reductions of ^{18}F-FDG uptake, measured either by SUV-max (black boxes) or SUV-mean (white boxes), during the study. Boxes represent interquartile distribution. Horizontal bars within boxes are median values. Error bars are 10th and 90th percentiles.
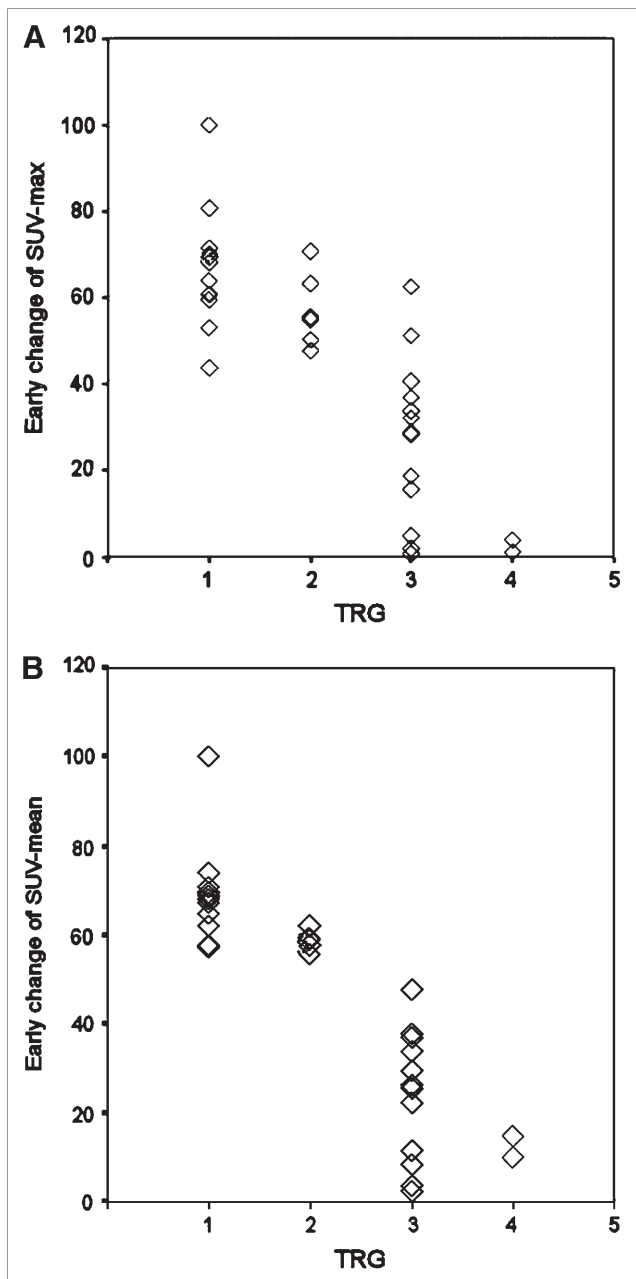
FIGURE 2. Early changes of SUV-max (A) and of SUV-mean (B) relative to TRG values.

comparisons). Representative PET images and measured SUV values in a nonresponder and a responder patient are given in Figures 3 and 4, respectively.

Using ROC analysis (Fig. 5), a 100% overall accuracy was shown for the early change of SUV-mean applying a cutoff value of −52%, whereas the optimum threshold value for the SUV-max was −42%. Using this cutoff value, all responders and 13 of 15 nonresponders were identified (sensitivity, 100%; specificity, 87%; overall accuracy, 94%).

Conversely, the presurgical PET data demonstrated no statistically significant correlation between SUV-mean late

changes and the TRG findings ($P = 0.2$). Similarly, we observed a low correlation between overall changes and the TRG findings ($P = 0.63$).

DISCUSSION

To our knowledge, this is the first study showing that early ^{18}F-FDG PET changes predict the activity of preoperative radiochemotherapy in LARC patients, differentiating responding (TRG1 or TRG2) from nonresponding (TRG3 or TRG4) tumors, as early as 12 d after the beginning of treatment. Indeed, although the ^{18}F-FDG SUV decreased on each subsequent scan, the degree of reduction in glucose consumption observed after the first 2 wk of therapy was strictly related to the final pathologic response. On the other hand, baseline ^{18}F-FDG SUVs were extremely variable and unrelated to both the clinical characteristics and the pathologic findings. As a matter of fact, the lowest baseline SUV-mean values of the whole series were found in 2 patients showing a TRG4 after primary treatment (Table 1).

At 12 d from the beginning of therapy, the SUV decreased in all tumors, although this reduction was very small (<10%) in 3 cases. In no instance did we observe an increase in ^{18}F-FDG uptake in and surrounding the tumor at this early scanning time. Previous studies had raised concerns of possible increases in ^{18}F-FDG uptake in and around tumors early after radiation treatment that could possibly yield false-positive results. This was described in an early study (24) in which scans performed on patients with recurrent colorectal cancer shortly after combination treatment with traditional and neutron radiation therapy showed lower than expected reduction in ^{18}F-FDG uptake, which was attributed to inflammation secondary to radiation injury. This study, however, was performed with early-generation whole-body scanners with perhaps lower overall image quality than currently available, particularly in imaging the pelvis. Another study performed in animal tumor models showed that inflammatory cells within tumors contribute significantly to the overall uptake of ^{18}F-FDG (25). Furthermore, studies performed in cell culture models show a transient increase in ^{18}F-FDG uptake in cancer cells shortly after irradiation (26). On the other hand, Schiepers et al. showed that ^{18}F-FDG uptake on PET scans performed within 2 wk from the end of a 2-wk course of radiation treatment was significantly reduced and was correlated with the viable tumor volume (27). On the basis of observations of previously published studies and our own results, we hypothesize that nonspecific ^{18}F-FDG accumulation during chemo- or radiotherapy is likely to have minimal impact and may be affected by the timing of the PET scan. In our series, we found significant reduction in tumor ^{18}F-FDG uptake and no interference by inflammatory or other nonspecific phenomena in PET scans performed 12 d after the beginning of treatment.

The main finding of this study is that early changes in SUV-mean accurately predict the pathologic findings in

FIGURE 3. Time course of ^{18}F-FDG PET in a nonresponder patient (patient 1). (A) Intense ^{18}F-FDG uptake in baseline study clearly depicts irregular tumor mass. (B) Tumor uptake is roughly unchanged in intermediate study (early SUV change, −15%). (C) In presurgical study, tumor volume is reduced but considerable tumor uptake is still present (late SUV change, −23%). This case was graded TRG4.
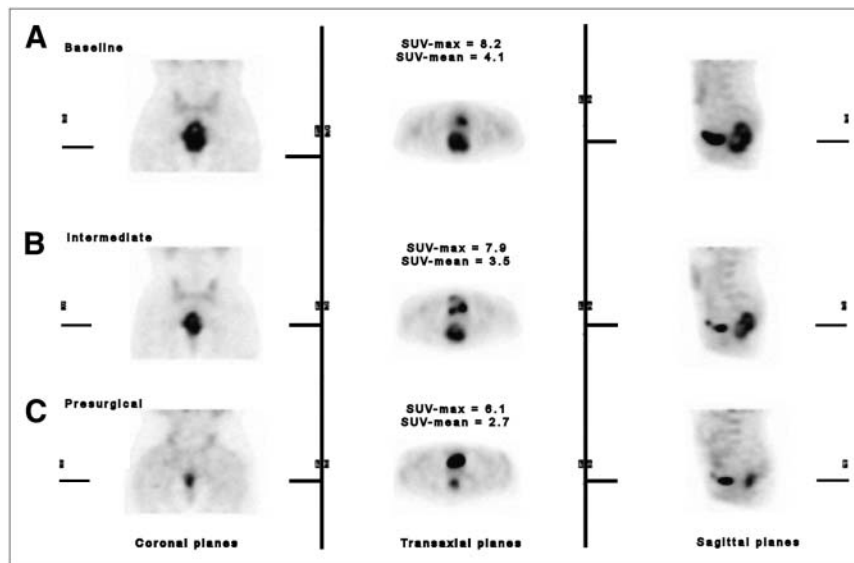
LARC, although a high statistical significance was observed also for SUV-max. In fact, as shown by ROC analysis, a SUV-mean early decrease ≥ 52% correctly predicted all responder patients. Measurement of the SUV-mean most likely better reflects behavior of the entire tumor mass, where heterogeneity of tumor cells and of the architecture of the lesion (viable cells mixed to fibrosis or necrosis) must be considered. Similarly, the TRG estimates the viable tumor cells and coexisting fibrosis ratio. This observation may explain the high correlation between the early SUV-mean change and the TRG score findings.

Conversely, although preoperative PET scans were performed only on a limited number of patients, the data obtained from these scans were less predictive of the pathologic response and these findings affected the accuracy of overall and late SUV changes. In this light, our results are similar to those reported on advanced esophageal cancer (*17*) and further support the usefulness of performing ^{18}F-FDG PET early during preoperative radiochemotherapy of LARC. Indeed, we found a further reduction of ^{18}F-FDG SUV on all presurgical PET scans; however, in 5 patients classified as nonresponders, a late SUV decrease ≥ 50% was observed. Moreover, ^{18}F-FDG uptake was undetectable in the presurgical scan on 2 patients with a TRG3 or TRG4. The explanation for such low or undetectable ^{18}F-FDG tumor uptake might be related either to the low number of viable tumor cells within the lesion or to the background activity, increased by the radiation effects. Furthermore, the presence of "stunned" tumor cells late during the course of radiochemotherapy should also be considered.

FIGURE 4. Time course of ^{18}F-FDG PET in a responder patient (patient 31). (A) Intense ^{18}F-FDG uptake is evident on baseline scan in a T2 lesion. (B) Significant decrease of SUV is observed on the intermediate scan. Early SUV change was −62%. (C) Complete tumor disappearance is noted on presurgical scan. Subtotal tumor regression (TRG2) was achieved. Activity in left ureter can be seen on transaxial images. n.m. = not measurable.
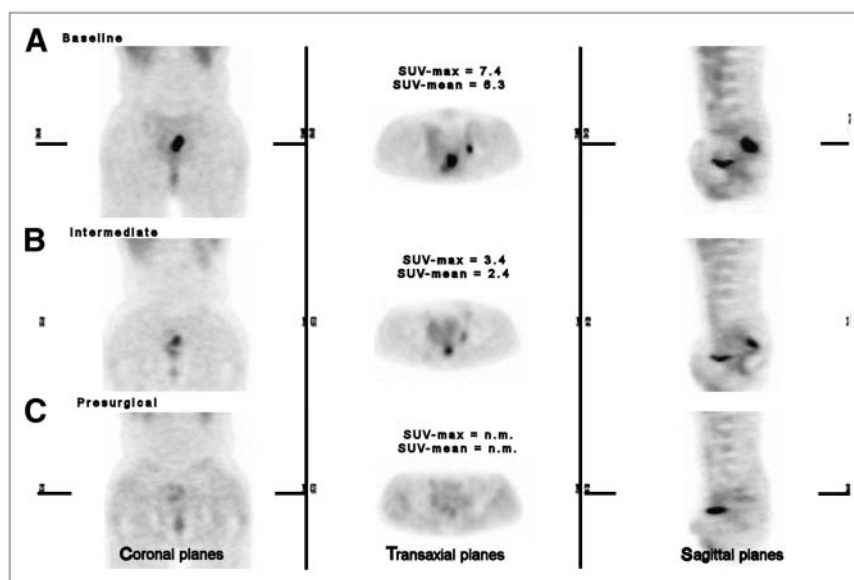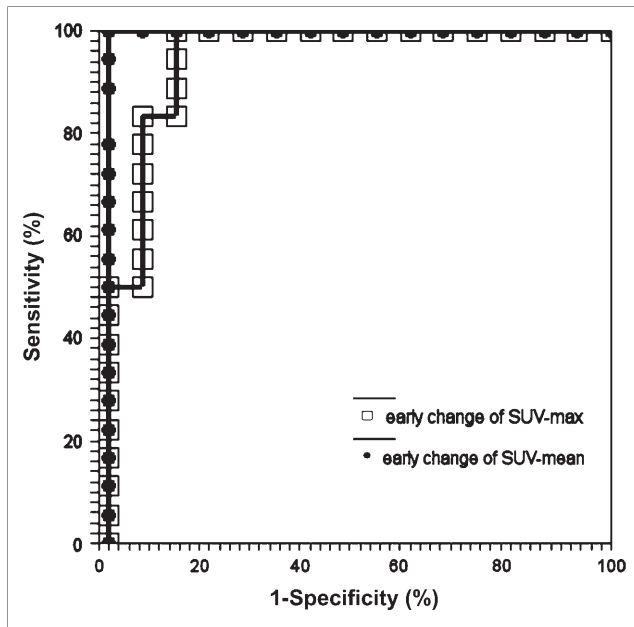
FIGURE 5. ROC curve analysis for early SUV changes in discriminating responder and nonresponder patients. Cutoff value in SUV-mean (closed circles) change of −52% yields values of 100% in sensitivity and specificity, whereas cutoff value in SUV-max (open boxes) of −42% gives a sensitivity of 100% and a specificity of 87% (area under curve, 0.95; confidence interval, 95%).

Other studies indicate a predictive value of presurgical ^{18}F-FDG PET on pathologic response assessed as a reduction of at least 1 T level (28–32). In this regard, it should be noted that the pTNM system may be inadequate for assessing response, as it only considers the location of residual tumor cells within the different strata of the rectum. Consequently, this classification does not differentiate between tumors harbored within the same stratum having gross or minimal residual disease. Conversely, the TRG-based assessment provides a more uniform method of evaluation, as it considers both the amount of residual tumor cells and the presence of fibrosis (18).

Finally, it is of interest to note that a recent study evaluating the predictive value of gene expression profiling on preoperative biopsies of LARCs through sophisticated molecular analyses (33) has yielded lower accuracy compared with our current ^{18}F-FDG PET findings. Given the dynamic induction of drug resistance mechanisms by preoperative radiochemotherapy, the ability to adequately predict response requires longitudinal analysis (34). In this respect, PET is a powerful predictive tool as it can evaluate changes of metabolic activity in the entire tumor mass and it gives the possibility of easily performing multiple determinations for detailed longitudinal analyses.

CONCLUSION

The early prediction of the pathologic findings by ^{18}F-FDG PET might play a relevant role in the management of LARC patients with preoperative radiochemotherapy. Indeed, early SUV changes may identify patients in whom neoadjuvant treatment will be ineffective, thus allowing alternative treatment strategies to be undertaken while sparing the cost and side effects of a useless therapy. On the other hand, early identification of patients in whom a complete or subtotal tumor regression—which is usually associated with a low prevalence of nodal involvement (18,35)—will be achieved may allow the surgeon to plan a more conservative approach, such as sphincter saving and local excision procedures.

REFERENCES

1. NIH Consensus Conference. Adjuvant therapy for patients with colon and rectal cancer. *JAMA.* 1990;264:1444-1450.
2. Enker WE. Total mesorectal excision: the new golden standard of surgery for rectal cancer. *Ann Med.* 1997;29:127–133.
3. Kapiteijn E, Marijnen CA, Nagtegaal ID, et al. Preoperative radiotherapy combined with total mesorectal excision for resectable rectal cancer. *N Engl J Med.* 2001;345:638–646.
4. MacFarlane JK, Ryall RD, Heald RJ. Mesorectal excision for rectal cancer. *Lancet.* 1993;341:457–460.
5. Minsky BD, Cohen AM, Kemeny N, et al. Enhancement of radiation-induced downstaging of rectal cancer by fluorouracil and high-dose leucovorin chemotherapy. *J Clin Oncol.* 1992;10:79–84.
6. Rodel C, Grabenbauer GG, Schick C, Papadopoulos T, Hohenberger W, Sauer R. Preoperative radiation with concurrent 5-fluorouracil for locally advanced T4-primary rectal cancer. *Strahlenther Onkol.* 2000;176:161–167.
7. Sauer R, Becker H, Hohenberger W, et al. Preoperative versus postoperative chemoradiotherapy for rectal cancer. *N Engl J Med.* 2004;351:1731–1740.
8. Beets-Tan RG, Beets GL, Vliegen RF, et al. Accuracy of magnetic resonance imaging in prediction of tumour-free resection margin in rectal cancer surgery. *Lancet.* 2001;357:497–504.
9. Brown G, Davies S, Williams GT, et al. Effectiveness of preoperative staging in rectal cancer: digital rectal examination, endoluminal ultrasound or magnetic resonance imaging? *Br J Cancer.* 2004;91:23–29.
10. Marijnen CA, Nagtegaal ID, Kapiteijn E, et al. Radiotherapy does not compensate for positive resection margins in rectal cancer patients: report of a multicenter randomized trial. *Int J Radiat Oncol Biol Phys.* 2003;55:1311–1320.
11. Chen CC, Lee RC, Lin JK, Wang LW, Yang SH. How accurate is magnetic resonance imaging in restaging rectal cancer in patients receiving preoperative combined chemoradiotherapy? *Dis Colon Rectum.* 2005;48:722–728.
12. Rau B, Hunerbein M, Barth C, et al. Accuracy of endorectal ultrasound after preoperative radiochemotherapy in locally advanced rectal cancer. *Surg Endosc.* 1999;13:980–984.
13. Garcia-Aguilar J, Hernandez de Anda E, Sirivongs P, Lee SH, Madoff RD, Rothenberger DA. A pathologic complete response to preoperative chemoradiation is associated with lower local recurrence and improved survival in rectal cancer patients treated by mesorectal excision. *Dis Colon Rectum.* 2003; 46:298–304.
14. Ruo L, Tickoo S, Klimstra DS, et al. Long-term prognostic significance of extent of rectal cancer response to preoperative radiation and chemotherapy. *Ann Surg.* 2002;236:75–81.
15. Schelling M, Avril N, Nahrig J, et al. Positron emission tomography using [18F]fluorodeoxyglucose for monitoring primary chemotherapy in breast cancer. *J Clin Oncol.* 2000;18:1689–1695.
16. Swisher SG, Erasmus J, Maish M, et al. 2-Fluoro-2-deoxy-D-glucose positron emission tomography imaging is predictive of pathologic response and survival after preoperative chemoradiation in patients with esophageal carcinoma. *Cancer.* 2004;101:1776–1785.
17. Wieder HA, Brucher BL, Zimmermann F, et al. Time course of tumor metabolic activity during chemoradiotherapy of esophageal squamous cell carcinoma and response to treatment. *J Clin Oncol.* 2004;22:900–908.
18. Vecchio FM, Valentini V, Minsky BD, et al. The relationship of pathologic tumor regression grade (TRG) and outcomes after preoperative therapy in rectal cancer. *Int J Radiat Oncol Biol Phys.* 2005;62:752–760.
19. Gunderson LL, Sargent DJ, Tepper JE, et al. Impact of T and N stage and treatment on survival and relapse in adjuvant rectal cancer: a pooled analysis. *J Clin Oncol.* 2004;22:1785–1796.

20. Avallone A, Delrio P, Guida C, et al. Biweekly oxaliplatin, raltitrexed, 5-fluorouracil and folinic acid combination chemotherapy during preoperative radiation therapy for locally advanced rectal cancer: a phase I-II study. *Br J Cancer.* 2006;94:1809–1815.

21. Andreola S, Leo E, Belli F, et al. Adenocarcinoma of the lower third of the rectum surgically treated with a <10-mm distal clearance: preliminary results in 35 N0 patients. *Ann Surg Oncol.* 2001;8:611–615.

22. Andreola S, Leo E, Belli F, Gallino G, Sirizzotti G, Sampietro G. Adenocarcinoma of the lower third of the rectum: metastases in lymph nodes smaller than 5 mm and occult micrometastases—preliminary results on early tumor recurrence. *Ann Surg Oncol.* 2001;8:413–417.

23. Mandard AM, Dalibard F, Mandard JC, et al. Pathologic assessment of tumor regression after preoperative chemoradiotherapy of esophageal carcinoma: clinicopathologic correlations. *Cancer.* 1994;73:2680–2686.

24. Haberkorn U, Strauss LG, Dimitrakopoulou A, et al. PET studies of fluorodeoxyglucose metabolism in patients with recurrent colorectal tumors receiving radiotherapy. *J Nucl Med.* 1991;32:1485–1490.

25. Kubota R, Yamada S, Kubota K, Ishiwata K, Tamahashi N, Ido T. Intratumoral distribution of fluorine-18-fluorodeoxyglucose in vivo: high accumulation in macrophages and granulation tissues studied by microautoradiography. *J Nucl Med.* 1992;33:1972–1980.

26. Higashi K, Clavo AC, Wahl RL. In vitro assessment of 2-fluoro-2-deoxy-D-glucose, L-methionine and thymidine as agents to monitor the early response of a human adenocarcinoma cell line to radiotherapy. *J Nucl Med.* 1993;34:773–779.

27. Schiepers C, Haustermans K, Geboes K, Filez L, Bormans G, Penninckx F. The effect of preoperative radiation therapy on glucose utilization and cell kinetics in patients with primary rectal carcinoma. *Cancer.* 1999;85:803–811.

28. Amthauer H, Denecke T, Rau B, et al. Response prediction by FDG-PET after neoadjuvant radiochemotherapy and combined regional hyperthermia of rectal cancer: correlation with endorectal ultrasound and histopathology. *Eur J Nucl Med Mol Imaging.* 2004;31:811–819.

29. Calvo FA, Domper M, Matute R, et al. ^{18}F-FDG positron emission tomography staging and restaging in rectal cancer treated with preoperative chemoradiation. *Int J Radiat Oncol Biol Phys.* 2004;58:528–535.

30. Denecke T, Rau B, Hoffmann KT, et al. Comparison of CT, MRI and FDG-PET in response prediction of patients with locally advanced rectal cancer after multimodal preoperative therapy: Is there a benefit in using functional imaging? *Eur Radiol.* 2005;15:1658–1666.

31. Guillem JG, Puig-La Calle J Jr, Akhurst T, et al. Prospective assessment of primary rectal cancer response to preoperative radiation and chemotherapy using 18-fluorodeoxyglucose positron emission tomography. *Dis Colon Rectum.* 2000; 43:18–24.

32. Oku S, Nakagawa K, Momose T, et al. FDG-PET after radiotherapy is a good prognostic indicator of rectal cancer. *Ann Nucl Med.* 2002;16: 409–416.

33. Ghadimi BM, Grade M, Difilippantonio MJ, et al. Effectiveness of gene expression profiling for response prediction of rectal adenocarcinomas to preoperative chemoradiotherapy. *J Clin Oncol.* 2005;23:1826–1838.

34. Rau B, Sturm I, Lage H, et al. Dynamic expression profile of p21WAF1/CIP1 and Ki-67 predicts survival in rectal carcinoma treated with preoperative radiochemotherapy. *J Clin Oncol.* 2003;21:3391–3401.

35. Read TE, Andujar JE, Caushaj PF, et al. Neoadjuvant therapy for rectal cancer: histologic response of the primary tumor predicts nodal status. *Dis Colon Rectum.* 2004;47:825–831.